

Time-Stretched Short-Time Fourier Transform

Abul Nuruzzaman, Ozdal Boyraz, *Member, IEEE*, and Bahram Jalali, *Fellow, IEEE*

Abstract—The authors propose and demonstrate the time-stretched short-time Fourier transform (TS-STFT) technique to overcome the limitation of an analog–digital converter (ADC) in the time–frequency analysis of ultrafast signals. Experimentally, the time–frequency analysis of highly chirped RF signals, with a chirp rate as high as 350 GHz/ns, is demonstrated. An effective real-time sampling rate of 320 GSa/s is achieved. Time stretching enhances the analog bandwidth and the effective sampling rate of the ADC and enables measurement of the instantaneous behavior of highly nonstationary ultrawideband signals.

Index Terms—Analog–digital converter (ADC), optical analog–digital conversion, optical quantization, optical sampling, optical signal processing, photonic time stretching, short-time Fourier transform (STFT), time stretch.

I. INTRODUCTION

A SHORT-TIME Fourier transform (STFT) is a well-known method for the time–frequency analysis of nonstationary signals. In an STFT, the signal is segmented by applying a window to it. The width of this window must be short enough such that the signal inside the window is assumed to be stationary. The window size determines the temporal resolution of the time–frequency analysis and establishes how well a nonstationary event can be localized in time. Naturally, a very short window is desired when analyzing highly chirped signals and signals where a nonstationary event occurs over a short interval.

Since an STFT is performed in the digital domain, the sampling rate of the analog–digital converter (ADC) limits the shortest window that can be achieved and, hence, restricts the effectiveness of the time–frequency analysis. The proposed time-stretched STFT (TS-STFT) overcomes this limitation through analog signal processing, which is performed prior to the ADC. First, an ultrashort window is applied to the nonstationary signal. The ultrashort window is then stretched in time to allow its capture by the ADC. The Fourier transform is then performed in the digital domain as it would be performed in a conventional STFT.

In this paper, we propose and demonstrate the STFT concept by using the time-stretch technique. A time–frequency analysis is experimentally demonstrated on highly chirped RF signals with chirp rates as high as 350 GHz/ns. The effective real-time sampling rate achieved in these experiments is 320 GSa/s.

Manuscript received June 15, 2004; revised September 7, 2005. This work was supported by the Defense Advanced Research Projects Agency (DARPA) Photonic A/D Converter Technology (PACT) program.

A. Nuruzzaman and B. Jalali are with the Optoelectronic Circuits and Systems Laboratory, Department of Electrical Engineering, University of California, Los Angeles (UCLA), Los Angeles, CA 90095-1594 USA (e-mail: jalali@ucla.edu).

O. Boyraz is with the Electrical Engineering and Computer Science Department, University of California, Irvine, CA 92697 USA (email: oboyraz@uci.edu).

Digital Object Identifier 10.1109/TIM.2006.864246

To the best of our knowledge, these results establish a record in the time–frequency analysis of ultrafast signals. The TS-STFT concept enhances the temporal resolution and increases the bandwidth. The system can be used for measuring ultrafast phenomena and is compatible with highly repetitive single-shot applications.

II. CONCEPT

The tenet in the TS-STFT is that the STFT of a highly chirp ultrafast signal is performed by reducing its bandwidth to match the ADC's input bandwidth and sampling rate. Fig. 1 illustrates this concept using the Gabor sampling lattice. Fig. 1(a) represents a conventional STFT analysis, and Fig. 1(b) describes a TS-STFT analysis. The window size, which is represented by the width of the cell along the time axis, is stretched by a factor M in the TS-STFT. It should be noted that the area of a single sampling cell is determined by the uncertainty principle and, hence, remains the same in both cases. This operation increases the detectable frequency bandwidth in the Gabor sampling lattice by a factor of M .

The time-stretch function can best be performed in the optical domain [1]. Here, the RF signal is modulated onto a chirped optical carrier. The waveform is then stretched in time by subjecting it to a linear dispersion [1]. This technique may be achieved optically due to the availability of wideband low-loss dispersion in the optical domain.

Fig. 2 shows the block diagram of the optical TS-STFT system. Signal windowing and time stretching are performed in the optical domain. Sampling, quantization, and STFT are executed in the electrical domain. Sequentially, the nonstationary RF signal is encoded on linearly chirped short optical pulses. This step represents the windowing function in a conventional STFT. Then, optical pulses are stretched in the time domain to reduce the RF bandwidth. After an optical–electrical conversion by a photodetector, the signal is sent to a digitizer. A Fourier transform is performed on the captured data to extract the instantaneous frequency behavior.

III. TIME-STRETCH PROCESS

An intuitive approach to understand the time-stretch process is through the time–wavelength mapping representation. The time-stretch process consists of two steps. Step 1 is the time–wavelength ($t-\lambda$) mapping performed by the combination of the chirped optical pulse and the electrooptic modulator. In this step, a gate signal is created by dispersing (stretching) an ultrashort optical pulse in a dispersive medium like optical fibers. After the dispersion process, each temporal point across the pulse corresponds to a different frequency component. When the intensity of this chirped pulse is modulated by

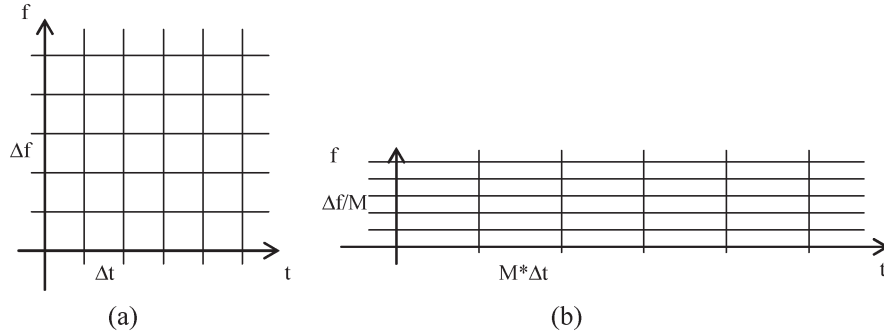


Fig. 1. Gabor sampling lattice of (a) STFT and (b) TS-STFT systems. Area of a single sampling cell in each picture is the same, but the time stretch increases the detectable frequency bandwidth of the STFT process. M is the stretch factor.

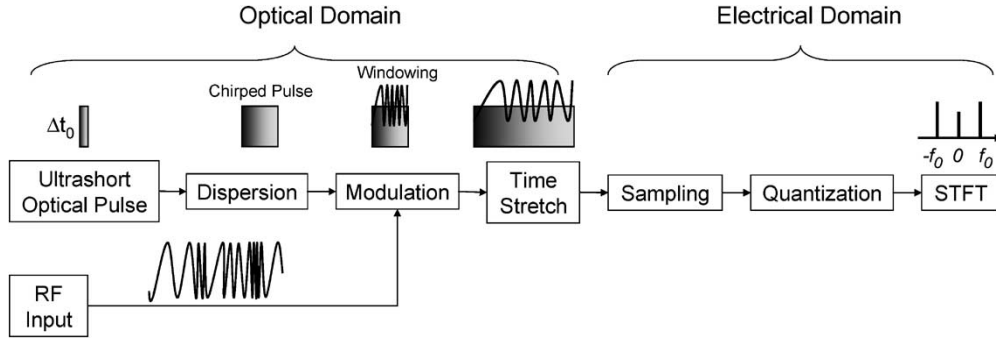


Fig. 2. Block diagram of the TS-STFT system.

an electrical signal after the stretching, the time–wavelength transformation is achieved. Step 2 is the wavelength–time (λ – t) mapping performed by the second dispersive medium followed by a photodetector. The modulated chirped pulse propagates through a second dispersive fiber. As a result, the temporal separation between individual frequency components increases; hence, the signal modulated onto the chirp pulse is stretched in the time. After the detection, a slowed-down representation of the high-frequency RF signal is obtained. A comprehensive and detailed treatment of the time-stretch theory can be found in [4].

To generate the chirped optical pulse, a nearly transform-limited ultrashort optical pulse needs to be linearly chirped after propagating through an optical dispersive medium. An optical fiber is a suitable dispersive medium, as it provides a reasonable dispersion over a broad bandwidth with a low loss. For applications where a low latency is required, a fiber Bragg grating (FBG) or an arrayed waveguide grating (AWG) can be used to generate the dispersion [2].

The validity of the time–wavelength representation can be understood through the following argument. Suppose that the chirped pulse is obtained by linearly dispersing a transform-limited pulse of the width Δt_o . This represents the system’s time resolution; in other words, time cannot be localized beyond Δt_o . Hence, the wavelength–time mapping picture is only valid when the time scale of interest is sufficiently larger than this time ambiguity. The time scale of interest depends on the speed of the electrical signal. The well-known Nyquist sampling theorem states that it is enough to sample a band-limited signal with the maximum frequency ω_{RF} at the sample interval of $\Delta T = \pi/\omega_{RF}$, without the loss of information. To map the time scale of an electrical signal with a frequency ω_{RF}

to an optical wavelength, it is required that $\Delta t_o \ll \pi/\omega_{RF}$. Fundamentally, Δt_o is related to the optical bandwidth ω_{opt} by the uncertainty principle $\omega_{opt}\Delta t_o \geq 1/2$. Relating optical and electrical bandwidths, the combination of uncertainty and Nyquist principles imply that the time–wavelength mapping representation is valid as long as $\omega_{RF} \ll 2\pi\omega_{opt}$. Typically, ω_{opt} is in the terahertz range, whereas ω_{RF} is in the gigahertz range. Therefore, the assumption is readily justified.

As described above, the time-stretch system relies on the linear group velocity dispersion (GVD) of the fiber characterized by the GVD parameter β_2 to linearly stretch the RF waveform in time. However, it is well known that the optical fiber possesses a nonlinear GVD, i.e., a GVD is a function of a wavelength. The wavelength dependence of a GVD is characterized by the higher order terms in the expansion of the mode propagation constant β as a function of the frequency, namely, β_3, β_4 , etc. [3]. A wavelength-dependent GVD may distort the RF signal since different time segments may be stretched by different amounts. In other words, the stretch factor can be time dependent. We have previously demonstrated that the nonlinear dispersion has no effect on the stretch factor in the time-stretch system [4]. This fortuitous effect occurs because the time–wavelength mapping in the two fibers counteract.

IV. EXPERIMENTAL SETUP AND RESULTS

The experimental setup of the TS-STFT system is shown in Fig. 3. A broadband optical supercontinuum generated in optical-pulse compression is used as an optical-pulse source [5]. After passing through a dispersion compensation fiber (DCF) module with $D1 = D * L1 = -116$ ps/nm, these pulses

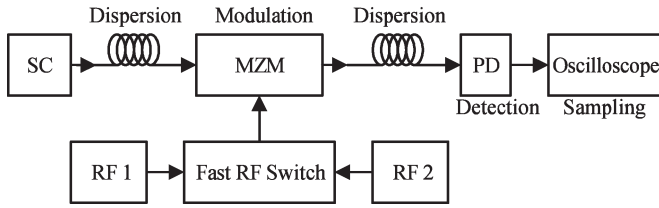


Fig. 3. Experimental setup of the TS-STFT system. Supercontinuum source (SC), Mach-Zehnder Modulator (MZM), Photodetector (PD), RF Signal 1 (RF1), and RF Signal 2 (RF2).

are used to window the incoming RF signal in a 2.3-ns time interval. To emulate an incoming highly chirped RF signal or a nonstationary signal, two high-frequency RF signals are time multiplexed by using a fast RF switch with a 25-ns switching time. The switch is synchronized to the pulse repetition rate of the laser (20 MHz) to ensure that the chirped RF signals overlap with the optical gating signal. The windowing of the chirped RF signal is performed by an electrooptic modulator when 2.3-ns segments of the RF signal are captured and modulated onto the optical pulses. The time stretching is performed by propagating the optical pulses through a second spool of DCF with a dispersion value of $D2 = D * L2 = -1740$ ps/nm. The stretch factor (M) is determined by the ratio of the dispersion in two DCF modules and expressed as $M = 1 + D2/D1 = 16$ [1]. The stretched envelope is then detected by a photodetector and captured by a real-time digital oscilloscope with a 20-GSa/s sampling rate and a 100- μ s memory length. The digitizer's memory allows us to capture 2000 consecutive single-shot events.

Fig. 4 shows the digitizer's output measurement, where 3.5–6-GHz RF signals are time multiplexed into the system. Through the time-stretch process, each pulse is stretched by the stretch factor of 16 and creates a time window of approximately 37 ns. As shown in the Fig. 4, 8 cycles of 3.5-GHz signals and 14 cycles of 6-GHz signals are encoded over a 2.3-ns time window and stretched to 37 ns. In the experiment, we use several combinations of two RF tones from 3 to 10 GHz to detect different chirp rates. A higher frequency limit is set by the dispersion penalty in the optical fiber. This phenomenon establishes a 3-dB bandwidth for the system and has been described elsewhere [4]. The detected RF pulses are processed in digital domain to eliminate the background noise and the envelope of the optical pulse. Fig. 5(a) shows the captured 6-GHz RF signal modulated on the optical signal and the envelope pulse without modulation. For the data processing, the optical-pulse envelope is removed from the signal in the time domain. To optimize the signal-to-noise ratio, a Hanning window is applied to the signal. Fig. 5(b) shows the 6-GHz intensity modulated signal after removing the envelope.

Fig. 6(a) and (b) show the frequency domain representation of the envelope-corrected 3.5- and 6-GHz signals, respectively. The spur-free dynamic range is 35.25 dB in Fig. 6(a) and 28.8 dB in Fig. 6(b). We achieve as high as 38.5 dB of dynamic range for the 3-GHz signal, which is limited by the noise floor of the oscilloscope. We find that the dynamic range is largely independent of the window size. As shown in Fig. 6, in addition to the harmonic peaks of the signal, several other peaks are

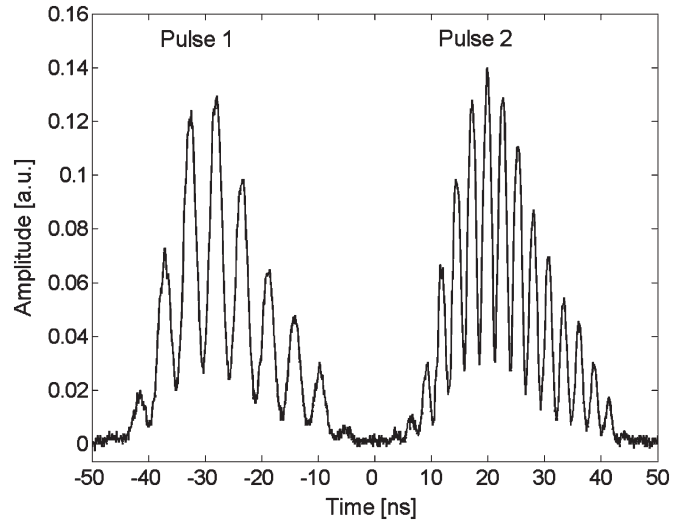


Fig. 4. Time-stretched 3.5- and 6-GHz RF captured by two consecutive optical pulses. Stretch factor = 16.

also observed. The origin of these peaks is in the nonuniform optical power spectrum. Through wavelength–time mapping, nonuniformities caused by the ripples of the optical bandpass filter are converted to a temporal modulation and result in spurs in the frequency domain.

V. DISCUSSION

State-of-the-art electronic oscilloscopes are not capable of capturing ultrafast RF signals let alone resolve their time–frequency behavior. With the availability of picosecond optical pulses, a TS-STFT allows us to place ultrashort windows on the RF signal. Additionally, time stretching slows down the windowed signal allowing it to be captured by a slow electronic digitizer. Combined, these two features enable us to study the instantaneous behavior of highly nonstationary waveforms.

In our experiment, we use the oscilloscope with a 4-GHz analog bandwidth and a 20-GSa/s maximum sampling rate. The use of the TS-STFT increased the sampling rate to 320 GSa/s (20 gigasample * stretch factor of 16). Additionally, we improve the analog bandwidth of the oscilloscope by 16 times, from 4 to 64 GHz. To process higher frequencies, the input bandwidth of the oscilloscope should be improved or the stretch factor M should be increased. Reducing the dispersion $D1$ or increasing the postmodulator dispersion $D2$ can increase the stretch factor. Typically, this will result in either a shorter time aperture of the system or a higher dispersion power penalty [1]. A single-sideband modulation has been proposed and demonstrated as a solution to this tradeoff [5], [6].

A practical limitation of the current experimental setup is the RF bandwidth of the electrooptical modulator. Although the oscilloscope can accept values as high as 64 GHz (after stretching) and the sampling rate is enough to resolve up to 160 GHz, the input frequency of the system is the 40-GHz RF bandwidth of the modulator. Ultimately, an optical modulator with a larger RF bandwidth is essential in order to unlock the vast potential of this technique.

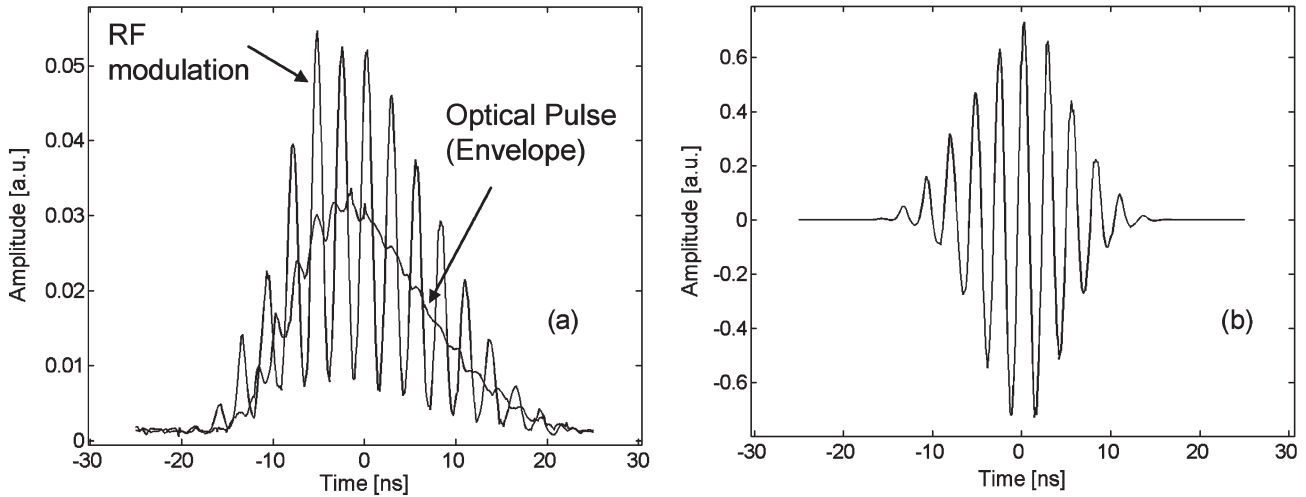


Fig. 5. (a) Six-GHz modulated signal with a static optical pulse and (b) 6-GHz modulated signal after the background correction (removal of the pulse envelope and Hanning windowing).

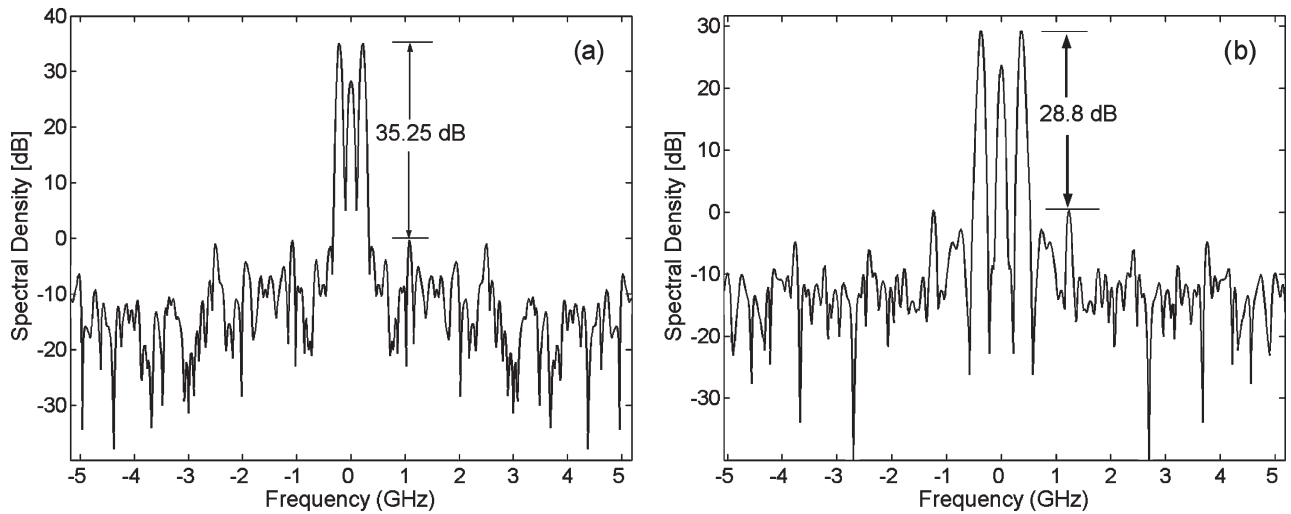


Fig. 6. RF spectra for captured (a) 3.5-GHz and (b) 6-GHz signals. Due to the stretch factor of 16, 3.5- and 6-GHz tones are observed at 219 and 375 MHz, respectively.

While the optical fiber is an effective medium for providing a large value of dispersion with a low loss, the latency associated with the propagation delay in the fiber may be undesirable in some applications. A low-latency time-stretch system can be realized using discrete-wavelength processing performed via optical filters. The discrete-time-stretch system is realized by replacing the fibers with a discrete-wavelength dispersive device, which is otherwise known as the wavelength-selective time delay [2]. Possible implementations include an array waveguide grating (AWG) in a loopback configuration [Fig. 7(a)] [7], [8] or fiber Bragg gratings [Fig. 7(b)]. For comparison, in the continuous-time system that uses fibers as the dispersive medium, a ~ 15 km of dispersion compensating fiber had to be used to generate a dispersion of -1740 ps/nm at 1585 nm (required to achieve a stretch factor of 16). This results in a latency close to $80 \mu\text{s}$, which is dictated by the pulse-propagating time. On the other hand, the latency in a discrete-wavelength stretch system is much lower. Assuming

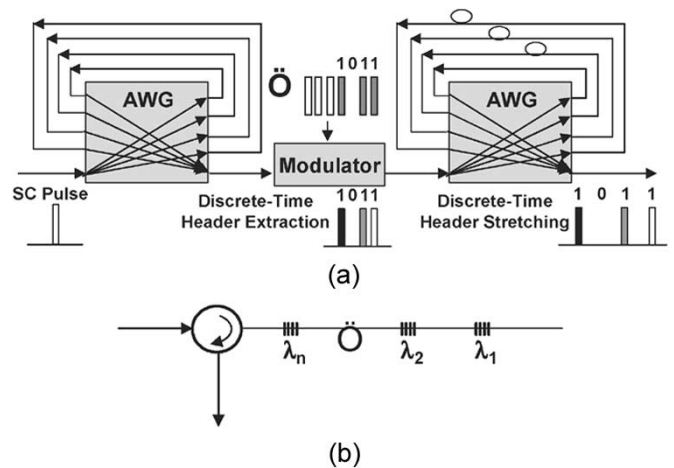


Fig. 7. Discrete-wavelength stretch system by (a) recirculating arrayed waveguide grating or (b) fiber Bragg gratings.

a configuration shown in Fig. 7(a), the main contribution to latency is the feedback delay in the feedback paths. Specifically, the latency is equal to the pulse-propagating time in AWGs and the longest delay in the feedback paths. For example, to realize a $16\times$ stretch factor with a 2.3-ns time window, the latency will be approximately < 50 ns. This is a drastic improvement compared to 80 μ s in the continuous-time system.

VI. SUMMARY

The authors experimentally resolve the instantaneous behavior of highly nonstationary RF signals with chirp rate of 350 GHz/ns and frequencies from 3 to 10 GHz. The highest dynamic range observed is 38.5 dB, limited by the noise floor of the digitizer. By slowing down the RF signal, the time-stretch technique enhances the sampling rate of the digitizer to a 320-GSa/s effective sampling rate.

REFERENCES

- [1] F. Coppinger, A. S. Bhushan, and B. Jalali, "Time magnification of electrical signals using chirped optical pulses," *Electron. Lett.*, vol. 34, no. 4, pp. 399–400, Feb. 1998.
- [2] Y. Han, O. Boyraz, and B. Jalali, "Optical header recognition using time stretch preprocessing," *Opt. Commun.*, vol. 237, no. 4–6, pp. 333–340, Jul. 15, 2004.
- [3] G. P. Agrawal, *Nonlinear Fiber Optics*, 3rd ed. New York: Academic, 2001, ch. 3.
- [4] Y. Han and B. Jalali, "Photonic time-stretched analog-to-digital converter: Fundamental concepts and practical considerations," *J. Lightw. Technol.*, vol. 21, no. 12, pp. 3085–3103, Dec. 2003.
- [5] A. S. Bhushan, P. V. Kelkar, B. Jalali, O. Boyraz, and M. N. Islam, "130-Gsa/s photonic analog-to-digital converter with time stretch preprocessor," *IEEE Photon. Technol. Lett.*, vol. 14, no. 5, pp. 684–687, May 2002.
- [6] J. M. Fuster, D. Novak, A. Nirmalathas, and J. Marti, "Single-sideband modulation in photonic time-stretch analogue-to-digital conversion," *Electron. Lett.*, vol. 37, no. 1, pp. 67–68, Jan. 2001.
- [7] A. S. Bhushan, F. Coppinger, S. Yegnanarayanan, and B. Jalali, "Nondispersive wavelength-division-sampling," *Opt. Lett.*, vol. 24, no. 11, pp. 738–740, Jun. 1999.
- [8] B. Jalali and S. Yegnanarayanan, "Method and apparatus for a wavelength selective true-time delay for an optically controlled device," U.S. Patent 5 793 907, Aug. 11, 1998.



Abul Nuruzzaman received the B.S. degree from Osaka University, Osaka, Japan, and the M.S. degree from the University of California, Los Angeles (UCLA), in 2002 and 2004, respectively, all in electrical engineering. He received the Japanese Ministry of Education "Monbusho" Scholarship to pursue his undergraduate degree in Japan from Bangladesh.

He is currently with Spansion, Flash Memory Division, Advance Micro Devices (AMD) Inc., Sunnyvale, CA, which is a Silicon Valley-based semiconductor company and with the Optoelectronic

Circuits and Systems Laboratory, Department of Electrical Engineering, UCLA.



Ozdal Boyraz (M'96) received the B.S. degree from Hacettepe University, Ankara, Turkey, in 1993 and the M.S. and Ph.D. degrees from the University of Michigan, Ann Arbor, in 1997 and 2001, respectively, all in electrical engineering.

From 2001 to 2003, he was an R&D Engineer at Xtera Communications, Allen, TX. In 2003, he joined University of California, Los Angeles (UCLA), as a Postdoctoral Research Scientist. In August 2005, he joined the Electrical Engineering and Computer Science Department, University of California, Irvine, as an Assistant Professor. He is the author of more than 60 scientific papers and is the holder of three U.S. patents with three applications pending.

Dr. Boyraz is a member of the IEEE Lasers and Electro-Optics Society (LEOS).



Bahram Jalali (S'86–M'89–SM'97–F'04) received the B.S. degree in physics from Florida State University, Tallahassee, in 1984 and the M.S. and Ph.D. degrees in applied physics from Columbia University, New York, NY, in 1986 and 1989, respectively.

From 1988 to 1993, he was a member of the Technical Staff at the Physics Research Division, American Telephone and Telegraph Company (AT&T) Bell Laboratories, Murray Hill, NJ. In 1993, he joined the Department of Electrical Engineering, University of California, Los Angeles (UCLA), where he is now

a Full Professor. He is the Director of the UCLA Optoelectronic Circuits and Systems Laboratory and the Director of the Consortium for Optical A/D System Technology (COAST): a national research center funded by the U.S. Department of Defense. He is the author or coauthor of more than 200 scientific papers and is the holder six U.S. patents with four applications pending. He was the Founder of Cognet Microsystems, which is a Los Angeles-based telecommunication components company, and served as its President, the Chief Executive Officer (CEO), and the Chair from the inception through the acquisition by Intel Corporation in 2001. He is a Senior Consultant to the Communication Group at Intel Corporation, Santa Clara, CA.

Prof. Jalali is a Full Member of the California NanoSystems Institute (CNSI). He is a Fellow of the Optical Society of America (OSA) and the Chair of the IEEE Lasers and Electro-Optics Society (LEOS) Los Angeles Chapter. He received the BridgeGate 20 Award for his contribution to the Southern California economy. His website can be found at <http://www.ee.ucla.edu/~simoecs/>.